

International Journal of Controls, Vol. 67, No. 1, 1997, pp. 89–116.

⁵Pachter, M., Chandler, P. R., and Mears, M., “Reconfigurable Flight Control with Saturation,” *Journal of Guidance, Control, and Dynamics*, Vol. 18, No. 5, 1995, pp. 1016–1023.

⁶Hess, R. A., and Snell, S. A., “Flight Control Design with Rate Saturating Actuators,” *Journal of Guidance, Control, and Dynamics*, Vol. 19, No. 1, 1996, pp. 38–46.

⁷Miller, R. B., and Pachter, M., “Maneuvering Flight Control with Actuator Constraints,” *Journal of Guidance, Control, and Dynamics*, Vol. 20, No. 4, 1997, pp. 729–734.

⁸Ngo, A. D., “Robust Control Design for Systems with Amplitude-Constrained Actuator,” Ph.D. Dissertation, Dept. of Aeronautics and Astronautics, Univ. of Washington, Seattle, WA, June 1999.

⁹Price, K., and Storn, R., “Differential Evolution,” *Dr. Dobb’s Journal*, Vol. 22, No. 4, 1997, pp. 18–22.

¹⁰Buffington, J. M., “Control Design and Analysis for Systems with Redundant Limited Controls,” Ph.D. Dissertation, Dept. of Control Science and Dynamical Systems, Univ. of Minnesota, Minneapolis, MN, March, 1996.

Simple Approach to East–West Station Keeping of Geosynchronous Spacecraft

T. S. No*

Chonbuk National University, Chonju 560-756,
Republic of Korea

Introduction

THE operation of geosynchronous (GEO) spacecrafts requires more precise and robust control of longitude drift because of the increase in the number of spacecrafts within the GEO orbit. As a result, the deadband of the station-keeping box for some GEO spacecrafts falls below ± 0.05 deg or less. A traditional approach to East–West (E/W) station keeping was that, at the time of crossing the deadband limit, the sign and the magnitude of the rate of mean longitude drift are restored to the predetermined values, and the magnitude and the direction of eccentricity vector are adjusted.^{1–4} This idea assumes that the long-term trend in orbit evolution that is due to the perturbations is fully predictable. However, the effects of perturbations such as luni-solar attraction and solar radiation pressure vary slightly from cycle to cycle and any maneuver error will propagate to the next cycle. Therefore enough margin should be reserved to ensure that the spacecraft longitude is maintained within the deadband, even in the presence of modeling uncertainty and maneuver execution errors.

In this Note, a simple variation of traditional E/W station keeping is proposed in which the predicted drift in mean longitude and eccentricity vector at the next maneuver time is used to find the target orbit for the current maneuver planning. The results of nonlinear simulation are presented to show that the spacecraft longitude is well maintained during the free-drift period.

Linearized Equations of Orbital Motions

Since the actual orbit of GEO spacecrafts is maintained near the geostationary orbit, its evolution may be described with the following set of station-keeping elements:

$$\Delta\lambda = \lambda - \lambda_s \quad (1)$$

$$\dot{\lambda} = \frac{dM}{dt} - \omega_e \quad (2)$$

$$e_x = e \cos(\Omega + \omega), \quad e_y = e \sin(\Omega + \omega) \quad (3)$$

where $\Delta\lambda$ denotes the longitude deviation from the nominal longitude λ_s , $\dot{\lambda}$ is the drift rate with respect to the Earth’s rotation rate ω_e , and $\mathbf{e} = (e_x, e_y)^T$ is defined as an eccentricity vector. Other symbols such as e , Ω , ω , and M represent the classical Keplerian orbit elements. If Eqs. (1–3) are substituted into the Lagrange planetary equations,⁵ after linearization one would get

$$\Delta\lambda(t) = [-3(\omega_e/V_{\text{syn}})\Delta V](t - \tau)\Delta t - \tau + \Delta\lambda(t) \quad (4)$$

$$\dot{\Delta\lambda}(t) = [-3(\omega_e/V_{\text{syn}})\Delta V]\Delta t - \tau + \dot{\Delta\lambda}(t) \quad (5)$$

$$\Delta e_x(t) = [(2/V_{\text{syn}})\Delta V \cos \alpha]\Delta t - \tau + \Delta e_x(t) \quad (6)$$

$$\Delta e_y(t) = [(2/V_{\text{syn}})\Delta V \sin \alpha]\Delta t - \tau + \Delta e_y(t) \quad (7)$$

where V_{syn} is the reference orbit speed, ΔV is the velocity increment that is due to the impulsive tangential thrusting, α is the sidereal angle of the spacecraft at the time τ of burn, and $\Delta t - \tau$ denotes the delta-Dirac function.

In Eqs. (4–7), $\Delta\lambda(t)$, $\dot{\Delta\lambda}(t)$, $\Delta e_x(t)$, and $\Delta e_y(t)$ represent the variations of station-keeping elements that are due to the natural perturbations acting on the GEO spacecrafts. One may numerically generate the time history of $\Delta\lambda(t)$, etc., by using the high-precision orbit propagator. If one considers their secular or long-term variations, analytical expressions could be found. A numerical technique may be used as it is known that the secular variations of $\Delta\lambda(t)$ can be well represented by a parabolic function and the mean eccentricity vector forms a circle with the period of 1 year.^{1–4} In this Note, the following expressions for $\Delta\lambda$ and $\Delta\mathbf{e}(t)$ are assumed:

$$\Delta\lambda(t) = p_1^\lambda \times 1 + p_2^\lambda \times t + p_3^\lambda \times (t^2/2) \quad (8)$$

$$\Delta\mathbf{e}(t) = p_1^e \times 1 + p_2^e \times \sin(\omega_s t) + p_3^e \times \cos(\omega_s t) \quad (9)$$

where ω_s denotes the sun’s rotation rate and the coefficients p_j^λ, p_j^e are determined with a least-squares curve fit.

Predictive Targeting and Fuel Optimal Transfer

The classical targeting strategy for E/W station keeping is that, at the time of maneuver, the secular drift rate of mean longitude is compensated for to restore the predetermined target value and the direction and the magnitude of mean eccentricity vector are adjusted so that they maintain certain geometrical relationships with respect to the sun vector. With reference to Fig. 1, the amount of compensation for the drift rate and eccentricity vector at the time of maneuver t_{NOW} may be written as

$$\dot{\Delta\lambda} = \dot{\lambda}_T - \dot{\lambda}(t_{\text{NOW}}) \quad (10)$$

$$\Delta\mathbf{e} = \mathbf{e}_T - \mathbf{e}(t_{\text{NOW}}) \quad (11)$$

where $\dot{\lambda}_T$ and \mathbf{e}_T are, respectively, the target drift rate and the eccentricity vector. If one is to use perigee-sun-tracking strategy for eccentricity control, the target for the eccentricity vector would be

$$\mathbf{e}_T = e_c \begin{bmatrix} \cos(\alpha_{\text{NOW}}^s - \alpha_{\text{EW}}) \\ \sin(\alpha_{\text{NOW}}^s - \alpha_{\text{EW}}) \end{bmatrix} \quad (12)$$

where α_{EW}^s is the sun’s right ascension at t_{NOW} , and α_{EW} , the sun lag angle, e_c , the maximum allowable eccentricity, and $\dot{\lambda}_T$ are determined with consideration of the station-keeping cycle, T_{EW} , and the deadband budget allocation.¹ This approach is based on the assumption that the long-term trends in the variations of longitude and eccentricity vector drift will be identical or at least similar at each maneuver cycle. However, as the deadband limit gets narrower, the seasonal and short-term variations should be duly accounted for.

One possible remedy to the above problem is that the maneuver is executed so that the target orbit is achieved at the end of next free-drift period. In other words, as illustrated in Fig. 2, the target longitude and the eccentricity vector are set as follows:

Received 12 November 1998; revision received 27 January 1999; accepted for publication 25 February 1999. Copyright © 1999 by the American Institute of Aeronautics and Astronautics, Inc. All rights reserved.

*Assistant Professor, Department of Aerospace Engineering. Member AIAA.

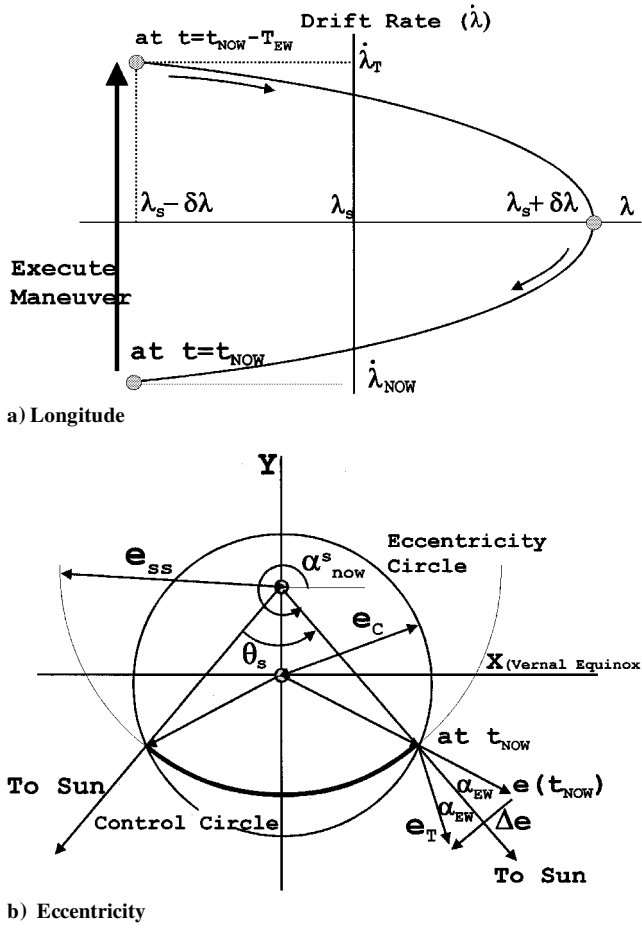


Fig. 1 Classical E/W station-keeping strategy.

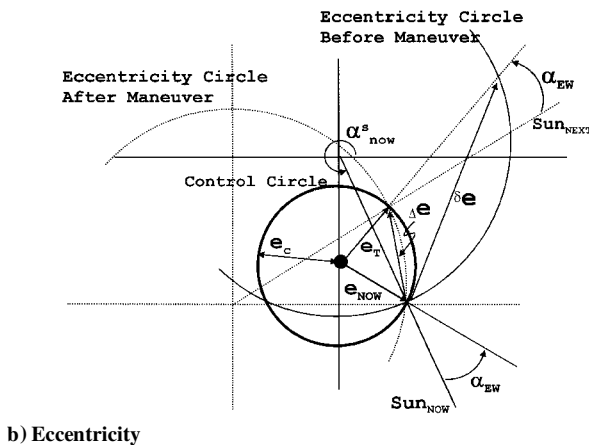
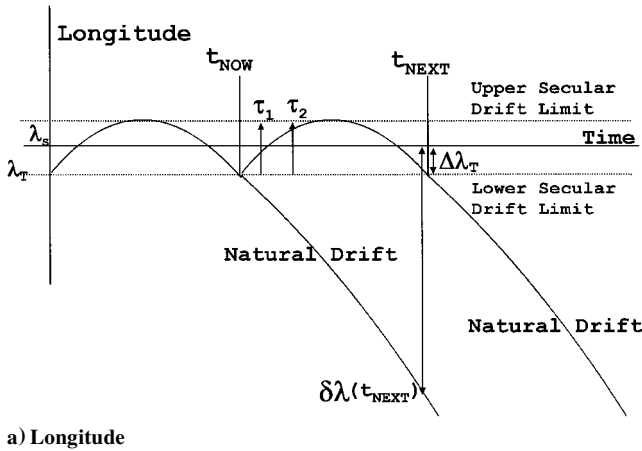


Fig. 2 Predictive E/W station-keeping strategy.

$\Delta\lambda_T$ = maximum permissible longitude deviation at the end of next free-drift period after the current maneuver

$$e_T = e_c \begin{bmatrix} \cos(\alpha_{NOW}^s + \alpha_{EW} + \omega_s \times T_{EW}) \\ \sin(\alpha_{NOW}^s + \alpha_{EW} + \omega_s \times T_{EW}) \end{bmatrix}$$

= target eccentricity vector at the end of next free-drift period after the current maneuver

If one uses the above conditions in conjunction with Eqs. (4), (6), and (7), one may find the N -impulse maneuver sequence by solving the following equations:

$$\Delta\lambda = \sum_{k=1}^N \left(-3 \frac{\omega_e}{V_{syn}} \Delta V_k \right) (t_{NEXT} - \tau_k) \Delta t_{NEXT} - \tau_k) + \Delta\lambda(t_{NEXT}) \quad (13)$$

$$\Delta e_x = \sum_{k=1}^N \left(\frac{2}{V_{syn}} \Delta V_k \cos \alpha_k \right) \Delta t_{NEXT} - \tau_k) + \Delta e_x(t_{NEXT}) \quad (14)$$

$$\Delta e_y = \sum_{k=1}^N \left(\frac{2}{V_{syn}} \Delta V_k \sin \alpha_k \right) \Delta t_{NEXT} - \tau_k) + \Delta e_y(t_{NEXT}) \quad (15)$$

where $t_{NEXT} (= t_{NOW} + T_{EW})$ and α_k denote, respectively, the time at the beginning of next station-keeping cycle and the sidereal angle of spacecraft at the time of k th burn. For the near-GEO orbit, α_k is related to the time as

$$\alpha_k = \omega_e (\tau_k - t_{vernal}) \quad (16)$$

where t_{vernal} is the latest time at the vernal equinox passage before the start of current station-keeping cycle. Also, $\Delta\lambda(t_{NEXT})$, $\Delta e_x(t_{NEXT})$, and $\Delta e_y(t_{NEXT})$ on the right-hand side of Eqs. (13–15) represent the longitude and the eccentricity vector drift that are due to the natural perturbations at the end of next station-keeping cycle if it were not for station-keeping maneuver. As stated above, these may be precisely predicted with the numerical integration and curve-fitting techniques.

For the multiple burn, viz., $N \geq 2$, the unique solution may not exist. Therefore one chooses the solution⁶ τ_k , ΔV_k , $k = 1, 2, \dots, N$, which minimizes the cost function

$$J = \sum_{k=1}^N |\Delta V_k| \quad (17)$$

and satisfies the constraints

$$t_{NOW} < \tau_1 < \tau_2 < \dots < \tau_N < t_{NEXT} \quad (18)$$

However, for practical reasons, the number of burns and the time between maneuver may be limited.

Numerical Examples

To show the validity of the predictive targeting strategy, a nonlinear numerical simulation was performed. A typical GEO spacecraft to be stationed at $116^\circ E \pm 0.05$ deg was chosen. But the deadband limit is further reduced to ± 0.033 deg and ± 0.017 deg is reserved for any possible errors. Other parameters used in the simulation are summarized in Table 1. For orbit perturbations, Earth gravity up to fourth order, sun/moon attraction, and solar pressure are considered in the nonlinear simulation. The number of impulses N was chosen to be 2, and burn time between maneuvers $|\tau_2 - \tau_1|$ was limited to 1 day. Then, one may find the maneuver sequence, that is, $(\tau_1, \Delta V_1)$ and $(\tau_2, \Delta V_2)$ by solving Eqs. (13–15) iteratively.

Table 1 Parameters used in the simulation

Nominal longitude λ_s	116°E
Station-keeping deadband	± 0.05 deg
Station-keeping cycle T_{EW}	7 days
Spacecraft area-to-mass ratio	$0.024 \text{ m}^2/\text{kg}$
Maximum eccentricity e_c	0.000235
Sun lag angle α_{EW}	3.97 deg

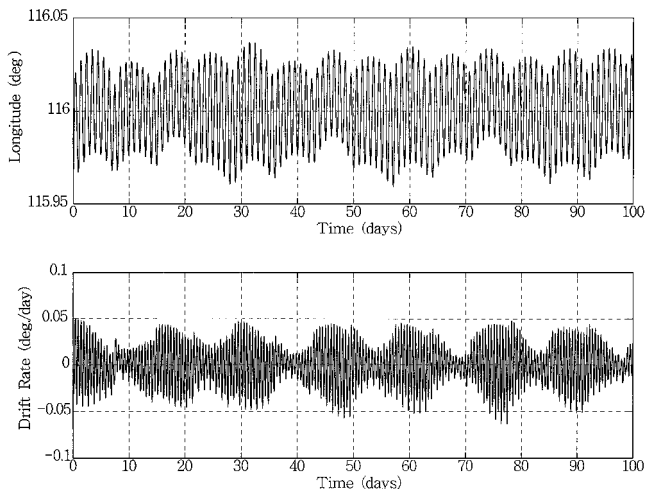
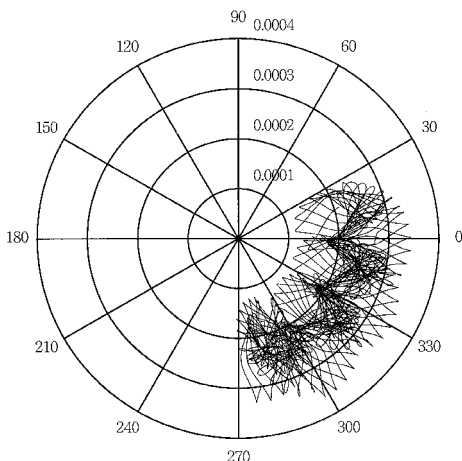
**a) Longitude****b) Eccentricity vector****Fig. 3 Nonlinear simulation results.**

Figure 3 displays the time history of longitude drift and the eccentricity vector for approximately 100 days. It is clear that the spacecraft is effectively maintained near its drifting toward the target conditions at the next station-keeping cycle, not from the conditions at the current cycle. Also, the longitude angle itself instead of drift rate is used in obtaining the target conditions. As a result, the spacecraft longitude could be controlled in a more precise and robust manner in the presence of modeling or maneuver execution errors.

Conclusions

In this Note, a predictive targeting strategy for E/W station keeping of GEO spacecrafts was presented and its performance verified in the nonlinear simulations. The important difference from the previous methods is that the spacecraft starts its drifting toward the target conditions at the next station-keeping cycle, not from the conditions at the current cycle. Also, the longitude angle itself instead of drift rate is used in obtaining the target conditions. As a result, the spacecraft longitude could be controlled in a more precise and robust manner in the presence of modeling or maneuver execution errors.

Acknowledgment

This work was supported by Korea Telecom under project control No. 97-18.

References

- ¹Pocha, J. J., *An Introduction to Mission Design for Geostationary Satellite*, Reidel, Dordrecht, The Netherlands, 1987, Chap. 6.
- ²Shrivastava, S. K., "Orbital Perturbations and Stationkeeping of Communication Satellites," *Journal of Spacecraft*, Vol. 15, No. 2, 1978, pp. 67-78.
- ³Kamel, A. A., and Ekman, D. E., "On the Orbital Eccentricity Control of Synchronous Satellites," *Journal of the Astronautical Sciences*, Vol. 30, No. 1, 1982, pp. 61-73.
- ⁴Kamel, A. A., "Geosynchronous Satellite Perturbations Due to Earth's Triaxiality and Luni-Solar Effects," *Journal of Guidance, Control, and Dynamics*, Vol. 5, No. 2, 1982, pp. 189-193.
- ⁵Chotov, V. A. (ed.), *Orbital Mechanics*, 2nd ed., AIAA Education Series, AIAA, Washington, DC, 1996, Chap. 9.
- ⁶No, T. S., "Fuel Optimal Multi-Impulse Orbit Rendezvous Between Neighboring Orbits: A Numerical Approach," *Advances in the Astronautical Sciences*, AAS 97-646, Vol. 97, Pt. 1, 1998, pp. 707-718.

Robust Fault Diagnosis for a Class of Linear Systems with Uncertainty

Bin Jiang,* Jian Liang Wang,† and Yeng Chai Soh†
Nanyang Technological University,
Singapore 639798, Republic of Singapore

I. Introduction

THE process of detection and isolation of system faults has been of considerable interest during the past two decades. Fruitful results can be found in several excellent survey papers.¹⁻⁶ Research is still under way into the development of more effective solutions for fault detection and isolation (FDI) in automatic control systems.

The model-based FDI concept is always under a number of idealized assumptions. Among them is that the mathematical model of the process is exactly known. In practice, this assumption can never be perfectly satisfied, as an accurate mathematical model of a physical process is never available. Because of this, there is often a mismatch between the actual process and its mathematical model, even if no fault in the process occurs. Such a mismatch causes fundamental methodological difficulties in FDI applications. They are a source of false alarms that can corrupt the performance of the FDI system.

To overcome the difficulty, FDI systems have to be made robust, i.e., insensitive or even invariant to such modeling errors or disturbances. A system designed to provide both sensitivity to faults and robustness to modeling error or disturbances is called a robust FDI scheme.^{7,8} One of the most successful robust fault diagnosis approaches is the use of the disturbance decoupling principle. This can be done by use of unknown input observers.⁹⁻¹¹ But in some cases, such as unstructured uncertainties in the system, perfect decoupling is not possible, so robust observers are to be designed for FDI.

In this Note we consider the FDI problem for a class of linear systems with uncertainties. At first, the system is transformed into two subsystems. The first subsystem is decoupled from actuator fault and the other is affected by the fault, but its states can be measured directly. As a generalization of the observer design approach in Ref. 12, a robust observer design is proposed for FDI. By using the estimation of states with bounded accuracy, we can approximate

Received 22 October 1998; revision received 3 March 1999; accepted for publication 4 March 1999. Copyright © 1999 by the American Institute of Aeronautics and Astronautics, Inc. All rights reserved.

*Research Fellow, School of Electrical and Electronic Engineering, Nanyang Avenue.

†Associate Professor, School of Electrical and Electronic Engineering, Nanyang Avenue.